

20

Materials

21 L-malic acid, indomethacin, and EDTA disodium were gained from Shanghai
22 Aladdin Reagent Co., Ltd. (Shanghai, China). NH_4Cl , BaCl_2 , MnCl_2 , CaCl_2 , CrCl_3 ,
23 CoCl_2 , MgCl_2 , NiCl_2 , SnCl_2 , ZnCl_2 , KI , Na_2S , KF , Na_3PO_4 , $\text{Na}_2\text{S}_2\text{O}_3$, KSCN , Na_2SO_4 ,
24 NaCl , Na_2CO_3 , NaNO_3 , KBr , Na_2SO_3 , NaNO_2 , cysteine, phenylalanine, alanine,
25 methionine, glutathione, arginine, tyrosine, proline, tryptophan, threonine, aspartic
26 acid, asparagine, isoleucine, and glycine were purchased from Beijing Chemical Corp
27 (Beijing, China). Distilled deionized (DDI) water was obtained from a Millipore Milli-
28 Q-RO4 water purification system with a resistivity higher than $18 \text{ M}\Omega \text{ cm}^{-1}$ (Bedford,
29 MA, USA). Dialysis membranes with a MWCO of 500-1000 Da were obtained from
30 Beijing Solarbio Science & Technology Co., Ltd. (Beijing, China).

31

Apparatus

32 Transmission electron microscopy (TEM) study was performed in a JEOL JEM-
33 2100 (Tokyo, Japan) instrument operating at an accelerating voltage of 200 KV. Atomic
34 force microscope (AFM) images were obtained using an AFM Bruker MultiMode 8 in
35 the contact mode. UV-vis absorption spectra were recorded using a Puxi TU-1901 UV-
36 vis absorption spectrophotometer. Fluorescent (FL) spectra were operated with a F-280
37 FL spectrophotometer (Tianjin, China). Fourier transform infrared (FTIR) spectra were
38 recorded on Thermo Scientific Nicolet iS50 FTIR Spectrometer (US). X-ray
39 photoelectron spectrometer (XPS) data were obtained with an AXISULTRA DLD
40 electron spectrometer from Shimadzu Company using 300W Al $\text{K}\alpha$ radiation. All FL
41 images were collected with Zeiss LSM880 confocal laser-scanning microscope.

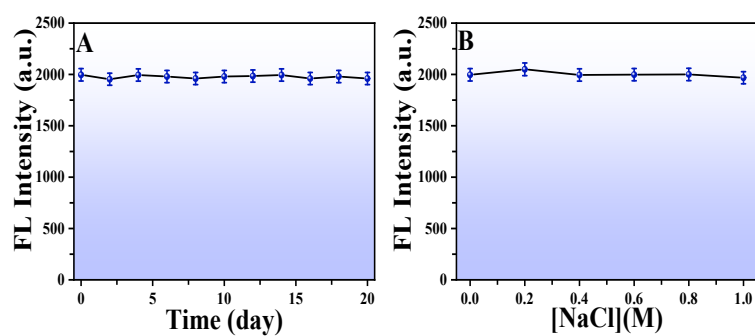
42

Detection Experiments in irrigation water

43 The detection ability of the B-CDs for Mn(VII) was evaluated in irrigation water.
44 The irrigation water sample is obtained from Shanxi University that were subjected to
45 recovery experiments. Fristly, Mn(VII) was determined by adding irrigation water
46 containing different concentrations of Mn(VII) (20, 50, 80, 120, 175, and 220 μM) to B-
47 CDs system, respectively. Then, the Mn(VII) concentrations were intelligently
48 quantified through YOLO v3 AI-driven smartphone monitoring platform.

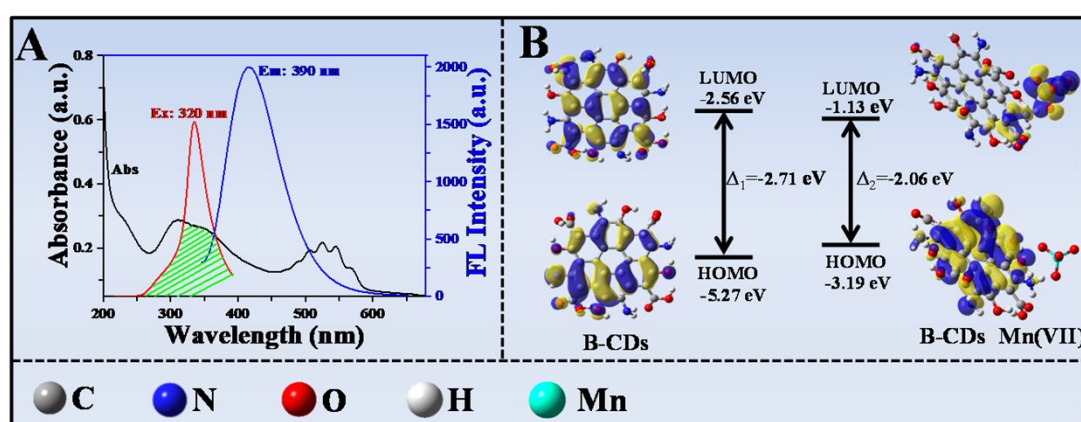
49

50



51

52 **Fig. S1** The effects of storage time (A) and NaCl concentration (B) on FL intensity of B-
 53 CDs.



54

55

56 **Fig. S2** (A) The overlap between absorption spectrum of Mn(VII) and the excitation-
 57 emission spectra of B-CDs. (B) Energy gap diagrams of HOMO and LUMO of B-CDs
 58 and before and after introducing Mn(VII).

64 **Fig. S4** Standard curves of Mn(VII) concentration fitted with different linear fitting
 65 algorithm based on (S+V)/H (Linear fitting algorithm: Least Squares, Ridge, Lasso,
 66 Lasso Lars, Bayesian Ridge, and SVM).

67 **Table S1** Comparison of different FL probes for Mn(VII) detection.

Fluorescence probes	Precursor	Linear range (μM)	LOD (nM)	Ref.
N-CDs	Threonine and guanidine hydrochloride	5–35	660	1
N-CDs	Citric acid, p-hydroxybenzoic acid and ammonia	0.51–2	170	2
N,S,P-CQDs	Saccharomyces cerevisiae	0.05–20	50	3
N,P-CDs	Phthalic acid, 1,2-ethylenediamine, and concentrated phosphoric acid	10–200	48.3	4
N,Al-CDs	Durian shell waste, urea, and aluminum nitrate	0–100	46.8	5
CDs	1,2-ethylenediamine, glucose and sulfuric acid	0.05–110	12.8	6
B-CDs	L-malic acid, indomethacin and EDTA disodium	1–270	7.5 nM	This work

68

69 **Table S2** Performance evaluation of the YOLO v3 algorithm.

Algorithmic model	Precision(%)	Recall(%)	F1-score(%)
YOLO v3	96.5	98.2	97.3

70

71

72

73 **References**

- 74 [1] A. Mohammed, Y. Gugulothu, R. Bandi, R. Dadigala, U.K. Utkoor, Ultraspeed
75 synthesis of highly fluorescent N-doped carbon dots for the label-free detection of
76 manganese(VII), *J. Chin. Chem. Soc-Taip.*, 2021, **68**, 1514–1521.
- 77 [2] V.M. Naik, D.B. Gunjal, A.H. Gore, P.V. Anbhule, D. Sohn, S.V. Bhosale, G.B.
78 Kolekar, Nitrogen-doped carbon dot threads as a “turn-off” fluorescent probe for
79 permanganate ions and its hydrogel hybrid as a naked eye sensor for gold(III) ions,
80 *Anal. Bioanal. Chem.*, 2020, **412**, 2993–3003.
- 81 [3] X. Gong, Z. Li, Q. Hu, R.X. Zhou, S.M. Shuang, C. Dong, N,S,P co-doped carbon
82 nanodot fabricated from waste microorganism and its application for label-free
83 recognition of manganese(VII) and L-ascorbic acid and AND logic gate operation,
84 *ACS Appl. Mater. Interfaces*, 2017, **9**, 38761–38772.
- 85 [4] F.F. Du, G. Li, X.J. Gong, Z.H. Guo, S.M. Shuang, M. Xian, C. Dong, Facile,
86 rapid synthesis of N,P-dual-doped carbon dots as a label-free multifunctional
87 nanosensor for Mn(VII) detection, temperature sensing and cellular imaging,
88 *Sensor. Actuat. B-Chem.*, 2018, **277**, 492–501.
- 89 [5] S. Jayaweera, K. Yin, X. Hu, W.J. Ng, Fluorescent N/Al co-doped carbon dots
90 from cellulose biomass for sensitive detection of manganese(VII), *J. Fluoresc.*,
91 2019, **29**, 1291–1300.
- 92 [6] Q. Hu, L.F. Liu, H.J. Sun, J. Han, X.J. Gong, L.Z. Liu, Z.Q. Yang, An ultra-
93 selective fluorescence method with enhanced sensitivity for the determination of
94 manganese(VII) in food stuffs using carbon quantum dots as nanoprobe, *J. Food*
95 *Compos. Anal.*, 2020, **88**, 103447–103455.